Soft Matter

Cite this: *Soft Matter*, 2012, **8**, 3363

www.rsc.org/softmatter

PAPER

Chemo-osmotically driven inhomogeneity growth during the enzymatic gelation of gelatin

Hayfa Souguir,[a] Olivier Ronsin,[a] Véronique Larreta-Garde,[b] Tetsuharu Narita,[c] Christiane Caroli[a] and Tristan Baumberger*[a]

Received 22nd November 2011, Accepted 11th January 2012
DOI: 10.1039/c2sm07234c

We present an extensive study of the enzyme-mediated, isothermal formation of covalently cross-linked gelatin gels. We find that the enzymatic activity in the forming network is drastically reduced compared with that in solution, and show that this can be attributed to the growing level of cross-link induced geometric constraints which impede translational and rotational motions. Thanks to the slowness of these kinetics, we monitor the concomitant build-up of the shear modulus G' and of the optical turbidity $\mathscr{T}$, which indicates that gelation is associated with the development of a high level of inhomogeneity. We find that, as the gelatin concentration c_G is varied, the levels of G' and $\mathscr{T}$ are strongly anti-correlated. Moreover, the lower c_G, the more precocious the emergence of $\mathscr{T}$. We are able to analyze inhomogeneity development in terms of the amplification of structural fluctuations *via* the coupling between the kinetics of the cross-linking reaction and the osmotic flow driven by swelling pressure fluctuations. We expect this positive feedback mechanism to be efficient in any slow, irreversible gelation process.

1 Introduction

Biopolymer gels, which were for several decades studied in view of their importance for the food industry, are presently the subject of intense additional interest as candidate materials for controlled drug release and scaffolds for tissue growth.[1] The propensity of many polysaccharides and proteins to self-assemble into (thermo- or iono-) reversible networks is indeed of obvious benefit in terms of bio-compatibility and degradability. But the other side of the coin is that, upon sustained use, such "physical" gels exhibit poor structural performance, due to the weakness of their cross-links. For this reason, interest is now increasingly focusing on introducing at least a small amount of covalent cross-links into the networks so as to optimize their mechanical properties.[2,3]

However, permanent gels raise two important questions:

- First, the addition of foreign chemical binders opens the question of possible pathogenic effects. An attractive, biomimetic solution to this problem is to resort to enzyme-mediated covalent cross-linking.

- The second issue is that of controlling the spatial scale and the amplitude of the network inhomogeneities, since biomedical applications have stringent requirements in terms of solute transport, hence of pore size distribution.

Studies of inhomogeneity distributions have essentially been concerned with the case when the cross-linking reaction is "instantaneous", *i.e.* very fast on the time scale of osmotic transport.[4] Here, on the contrary, we are interested in slow gelation kinetics: indeed, the cross-linking reactions of concern occur between residues sparsely distributed along the chains and require very specific relative orientations of the two moieties, particularly so in the case of enzymatic catalysis. Under such conditions, the question arises of a possible coupling between gelation and inhomogeneity growth kinetics. In order to shed some light on this fully open question, studies of the kinetics of inhomogeneity development during the course of gelation are clearly needed.

As a first step in this direction, we report here the results of an extensive study of isothermal gelation of aqueous gelatin solutions in the presence of a transglutaminase (Tgase), which catalyzes the formation of isopeptide covalent bonds between lysine and glutamine residues. Gelatin is well known to undergo, at temperatures below $T_g \approx 29\,^{\circ}C$, a coil-to-helix transition leading to physical gelation *via* the formation of triple helices.[5] It has been shown[6] that, for $T < T_g$, the presence of Tgase leads to the formation of gels containing a mixture of physical and chemical cross-links (CLs). In order to focus on pure chemical gels, all our experiments are performed at $T = 40\,^{\circ}C$, a temperature at which the gelatin chains remain in the coil state.[6]

[a]*Institut des nanosciences de Paris, Université Paris 6, UMR CNRS 7588, 2 place Jussieu, 75005 Paris, France. E-mail: tristan.baumberger@insp.jussieu.fr; Fax: (+33) 1 44 27 39 82; Tel: (+33) 1 44 27 78 62*
[b]*Equipe de Recherche sur les Relations Matrice Extracellulaire Cellules (Errmece), Institut des Matériaux, Cergy-Pontoise University, 95000 Cergy-Pontoise, France*
[c]*Laboratoire PPMD-SIMM, UMR7615, UPMC-ESPCI ParisTech-CNRS, 10 rue Vauquelin, 75005 Paris, France*

Enzyme mediated gelation is indeed very slow: completion is reached on a time scale of the order of days. While gelatin physical gels are always optically clear, our chemical gels are visually much more turbid (see Fig. 1). We monitor network formation *via* the evolution of the shear modulus G' and of the turbidity $\mathscr{T}$ for various values of the enzyme and gelatin concentrations, c_E and c_G. We find that the build-up of G' is systematically accompanied by that of $\mathscr{T}$. At fixed enzyme content c_E, the saturation modulus increases markedly with c_G. Moreover, we observe that, as c_G is varied, G' and $\mathscr{T}$ exhibit a strong anti-correlation: the smaller c_G, the larger $\mathscr{T}$ and the earlier its emergence with respect to elastic network percolation. This phenomenology is qualitatively reminiscent of that of agarose thermo-reversible gels,[7] which is now agreed to result from elastically arrested spinodal decomposition of the agarose/water mixture.[8,9] However the same mechanism cannot be invoked here, since gelatin solutions are well known to be thermodynamically stable down to their freezing temperature.

We propose an alternative interpretation in terms of chemo-osmotic dynamic coupling, already evoked by Nakazawa and Sekimoto[10] as a candidate mechanism for inhomogeneity amplification. It can be decomposed as follows: assume at some time the presence of a statistical fluctuation (*e.g.* an increase) of the CL density in an otherwise homogeneous gel; it induces *via* osmotic forces an increase of the local monomer density which, in turn, results in an increase of the cross-linking reaction rate in the same region, hence in the amplification of the initial fluctuation. We believe that this mechanism should be at work in any slow chemical polymer gelation. In order for it to result in a significant growth of the turbidity, the reaction kinetics should be slow enough to allow for the development of diffusive solute transport (microsyneresis) on length scales in the 100 nm range. Such appears to be the case for Tgase-mediated cross-linking of gelatin.

2 Materials and methods

Materials

Gelatin extracted from porcine skin by acidic processing (type A) was used as received. According to the supplier's (Sigma-Aldrich) specifications it has a Bloom[11] of 300 g, indicating an average molar mass $\bar{M}_w \simeq 90$ kDa. Its contents in lysine and glutamine + glutamic acid are, respectively, $\alpha_{Lys} = 2.6$ and $\alpha_{Gln} = 8.4$ (amino acids per 100 residues).[12] Its isoelectric point pI lies between 7 and 9.

Ca^{2+}-independent transglutaminase (Tgase) of microbial origin (*Streptovertcillium sp.*) was kindly supplied by Ajinomoto Foods Europe SAS under its commercial powder form (Activa-WM) in which the enzyme is mixed with an excipient (maltodextrine). It was kept at −20 °C until use, without further purification.

Tgase is a globular protein (65 Å × 59 Å × 41 Å) of molar mass approximately 38 kDa;[13] it catalyses a cross-linking reaction between the lateral chains of the glutamine and lysine residues of gelatin. It is active between pH 4 and pH 9. Its optimum temperature is 50 °C. It is inactivated after 10 min incubation at 70 °C.[14]

An enzymatic activity test was carried out using a small peptide—carbobenzyloxy-glutamylglycine (CBZ-Gln-Gly)—as a model substrate in the presence of hydroxylamine.[15] The specific activity of Activa-WM was 98 U g^{-1}†, in agreement with the supplier's specifications (81–135 U g^{-1}). The mass fraction of enzyme in the preparation was measured to be 0.5% by the Bradford colorimetric protein assay using Bovine Serum Albumine as a reference.[16] An enzyme unit (U) therefore corresponds to 1.3 nmol of Tgase. The above figures were subsequently used when calculating the amount of enzyme units in the gel samples.

We have checked, with the help of the SDS-PAGE test,[17] that Tgase was the main proteinic component of the preparation. Traces of protease were revealed by zymography,[18] carried out with a separating gel containing 0.1% of gelatin. Note that the amount of protease in the preparation was too small to induce any visible degradation in gels kept for months at ambient temperature.

Pregel preparation

Gelatin powder was dissolved under continuous stirring in ultrapure water (milli-Q) at 65 °C during 30 min, then kept at 40 °C. Sodium azide (500 ppm) was added in order to avoid bacterial contamination. Gelatin solutions have a pH = 5.1 ± 0.05 at 40 °C, almost independent of the gelatin concentration (3–10 wt%) indicating that gelatin has a buffer effect. This pH lies within the range of optimal activity for Tgase[14] and no other buffer solution was used in this study.

A Tgase solution in ultrapure water was prepared extemporaneously under magnetic stirring, then filtered through a 0.45 μm cellulose acetate membrane to remove excipient aggregates and kept at 40 °C for no more than 15 min before use. Pregels with concentrations in gelatin c_G (1.5–10 wt%) and enzyme c_E (0.25–2 U g^{-1}) were prepared by rapid mixing of appropriate volumes of enzyme and gelatin solutions. The whole homogenization phase, including ultrasonic degassing, lasted for 10 to 60 s depending on the viscosity of the pregel. Afterwards, it was quickly poured into cells adapted to rheological or optical measurements.

Unless otherwise specified, all measurements were performed at 40 ± 0.1 °C.

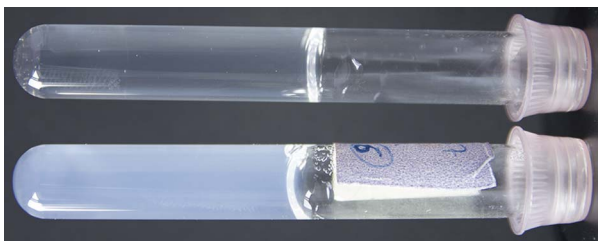

Fig. 1 Aspect of two gelatin gels with the same polymer content (5 wt%). Top: physically cross-linked at $T = 23$ °C. Bottom: chemically cross-linked by Tgase at $T = 40$ °C. Tube diameter: 1 cm.

† An enzyme unit is defined as the amount of enzyme which catalyses the synthesis of 1 μmole of product per minute under the specific test conditions.

Rheological tests

Viscoelastic properties of the gels in the linear regime were measured using a stress-controlled rheometer (Anton Paar, MCR 501) in the parallel plate geometry (50 mm diameter plates, sandblasted, 1 mm gap). All measurements were performed with 1% strain amplitude oscillations at 1 Hz. The samples were protected against water evaporation by a paraffin oil rim. Since this study deals with long experiments, lasting up to 3.5 days, solvent evaporation can be a serious issue. Indeed, using a silicon oil rim was found to lead to erratic torque fluctuations attributable to the formation of dry gel particles bridging the rheometer gap and yielding an apparent increase of the modulus, by as much as one order of magnitude. Since silicon oils are known to be much more permeable to water than mineral ones of comparable viscosity,[19] we have accordingly made use of a paraffin oil (kinematic viscosity $\gtrsim 45$ mm^2 s^{-1} at 40 °C) and checked that no spurious torque fluctuations were detectable, even for the longest experimental runs.

Turbidity

Measurements were carried out using an Ocean Optics USB 4000 spectrometer. The pregel was poured into a cuvette cell with $L =$ 1 cm optical path, placed in a thermostated holder and illuminated by the unpolarized light of a stabilized tungsten halogen source. Both the source and the spectrometer were coupled to the cuvette holder *via* optical fibers and collimating quartz lenses resulting in beam divergence and transmitted light collection angles $\lesssim 2$ deg. We monitor the transmitted intensity spectrum, from which we define the turbidity $\mathscr{T}(\lambda, t)$ as:

$$\mathscr{T}(\lambda, t) = -\frac{1}{L}\ln\left(\frac{I_t}{I_0}\right) \quad (1)$$

where L is the optical path, I_t the transmitted intensity at wavelength λ and time t, and I_0 its initial value, measured immediately after cell filling. Thus, $\mathscr{T}$ reflects the inhomogeneities of monomer concentration *induced by the cross-linking process*.

In order to simplify the discussion, we focused on a limited wavelength range (550–650 nm) over which the turbidity spectrum exhibits a quasi-power law behavior, and can therefore be fully characterized by two time-dependent parameters only, namely its value $\mathscr{T}^*$ at $\lambda = 630$ nm and the so-called wavelength exponent α defined as:

$$\alpha = \left.\frac{d\ln(\mathscr{T})}{d\ln(\lambda)}\right|_{550-650\text{nm}} \quad (2)$$

Within the framework of the Rayleigh–Debye theory for single scattering[20] α can be expressed as[7] $\alpha = -4 + \alpha_1 + \alpha_2 + d\ln(Q)/d\ln(\lambda)$, where α_1 stems from the dispersion of the medium and α_2 from its dependence on monomer concentration. These parameters are usually small and negative.[7] The spatial inhomogeneities of the monomer concentration are encoded in the last term *via* the structure factor $S(q)$. More precisely, the extinction factor Q reads:

$$Q(\lambda) = \int_{\theta_{min}}^{\pi} S(q).\left(1+\cos^2(\theta)\right)\sin(\theta)d\theta \quad (3)$$

where

$$q = \frac{4\pi n_0}{\lambda}\sin(\theta/2) \quad (4)$$

is the scattering vector at scattering angle θ in a medium of refractive index n_0, and $\theta_{\min} \simeq 2$ deg is the acceptance angle of the collimated optical fiber. In the absence of an accurate indication on the monomer distribution in the gel, we have computed numerically $\beta = d\ln(Q)/d\ln(\lambda)$ for a Lorentzian structure factor $S(q) = 1\Big/\left[1+(qd)^2\right]$ featuring a characteristic inhomogeneity length scale d. The resulting $\beta(d)$ curve is similar to that shown in Fig. 1 of Aymard *et al.*[7] as long as d is smaller than the average wavelength ($\simeq$650 nm) since, in this range, β does not depend significantly on the values of the (small) acceptance angles $\theta_{\min}$.

Weakly turbid gels display values of $\alpha \gtrsim -4.1$, from which we extract a conservative estimate for $\alpha_1 + \alpha_2 \simeq -0.1$ close to that obtained for agar gels.[7] Hence the calculated relation $\beta(d)$ could be inverted and yield d estimates from the measured α values.

Dynamic light scattering (DLS)

The measurements were performed at 40 °C with a ALV/CSG-3 System comprising a compact goniometer system and a multi-τ real-time digital correlator (ALV-GmbH, Langen, Germany), equipped with a cuvette rotation/translation unit (CRTU) and a He–Ne laser (22 mW at $\lambda = 632.8$ nm). The system measures the time-averaged autocorrelation function of the scattered light intensity at a scattering vector q:

$$g^{(2)}(\tau) \equiv g^{(2)}_T(\tau; q) = \frac{\langle I(0;q)I(\tau;q)\rangle_T}{\langle I(0;q)\rangle^2_T} \quad (5)$$

In order to circumvent the non-ergodicity associated with the presence of frozen disorder in the gel phase,[21] the sample cell is rotated steadily while *time* averaging. Thus, $g^{(2)}$ coincides with the ensemble-averaged autocorrelation function, up to a cut-off delay time fixed by the sample rotation speed.[22] The averaging duration was 50 s. In order to ensure that the system did not evolve over the duration of measurement, each sample was directly prepared in a light scattering cell and incubated at 40 °C for a prescribed time after which the enzyme was inactivated (see "materials" above). The sample was then kept at 40 °C prior to measurement. We have checked that our storage delays, up to 1 day after inactivation, do not affect the structure, by comparing the $g^{(2)}$ values with those measured during gelation on systems "old" enough for their turbidity to remain quasi-constant over 50 s.

In order to keep multiple scattering to an acceptable level, we have restricted measurements to systems with turbidity $\mathscr{T}^* < 0.1$ cm^{-1}. As will appear clearly in section 3, this strong requirement limits in practice the application of DLS to gels with $c_G \geq 5\%$ at relatively early stages of their cross-linking process.

Within these limits we found that the relaxation spectrum of the gels exhibited a diffusive mode signalled by

$$[g^2(\tau) - 1]^{1/2} = A\,\exp(-\tau/\tau_{\text{diff}}) + B \quad (6)$$

where A is a parameter that depends on the instrument coherence factor, and B stems from the long-lived correlations resulting from the frozen disorder, and

$$\tau_{\mathrm{diff}}^{-1} = D_{\mathrm{coll}} q^2 \quad (7)$$

D_{coll} is the network/solvent (also called "collective") diffusion coefficient.[23] The quadratic q-dependence of eqn(7) was checked to ensure that it was accurately obeyed for scattering angles between 30 and 150 deg corresponding to real-space lengths $2\pi/q$ between 250 and 900 nm. This indicates that when probed at this scale, our weakly turbid gels look homogeneous, *i.e.* monomer concentration fluctuations occur at smaller scales and are averaged-out by the light scattering process.

3 Results

3.1 Kinetics of shear modulus build-up

Fig. 2 shows a typical example of the growth of the storage modulus $G'(t)$ along the course of the gelation process, here measured for gelatin and enzyme concentrations $c_G = 5$ wt%, $c_E = 2$ U g^{-1}. t is defined as the time elapsed since the instant of mixing of the enzyme and gelatin solutions. Gelation is slow: network percolation, giving rise to a measurable modulus on the order of 1 Pa, occurs after about 1000 s. We define this gelation time t_0 more precisely as corresponding to the maximum of the loss modulus $G''(t)$ (see insert)—a feature present in all experimental runs‡. For $t > t_0$, G' builds up over more than two time decades before saturating. The system thus obtained is a *bona fide* chemical gel: its storage and loss moduli are constant over decades of frequency (typically 0.01–10 Hz), and its loss angle remains $\lesssim 10^{-3}$ (one order of magnitude smaller than that for physical gelatin gels).

Effect of enzyme concentration. We analyze it here in detail for systems with a fixed gelatin content $c_G = 5\%$. Fig. 3 displays the evolution of G' for different values of c_E, from 0.5 to 2 U g^{-1}. As expected, the larger the enzyme content, the faster gelation proceeds. This qualitative observation can be made more precise by measuring $t_0(c_E)$. Having in mind the fact that the cross-linking reaction involves a single, non consumed, enzyme (E) molecule, we tentatively plot t_0^{-1} *vs* c_E. In agreement with previous findings by Giraudier and Larreta-Garde,[24] the data shown in Fig. 4 is seen to obey a linear scaling relation quite satisfactorily.

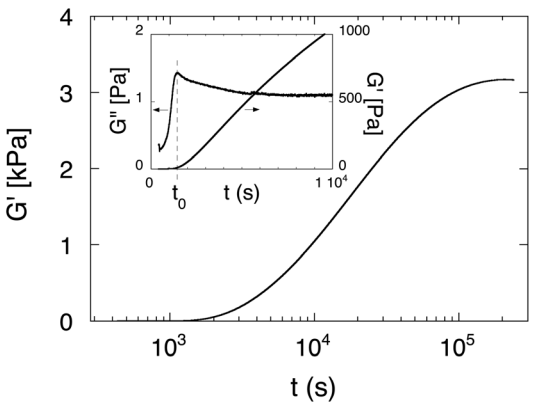

Fig. 2 Shear modulus *vs.* time during enzyme-mediated gelation of a $c_G = 5$ wt %, $cE = 2$ U g^{-1}. sample. Inset: blow-up of the storage (G') and loss (G'') moduli in the vicinity of the gelation time t_0 (see text).

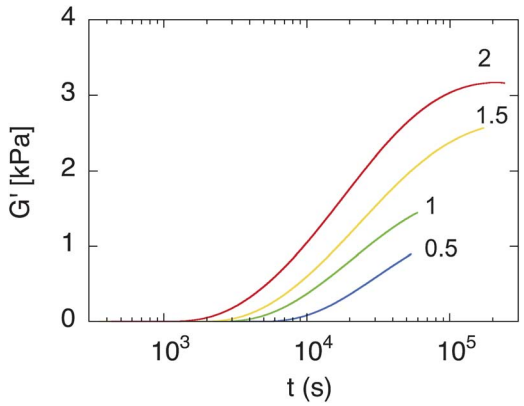

Fig. 3 Storage modulus build-up for gels with gelatin mass fraction $c_G = 5\%$ and enzyme contents as labelled (in U g^{-1}).

From this result, we deduce that, for this gelatin concentration, the state of the network at percolation is independent of the rate of the cross-linking reaction, which is itself set by a kinetics of first order in E. In other words, in the early stage of gelation at least, changing c_E would not affect the structure of the network, but only the pace at which it is constructed. In order to test the extent of this early regime, we plot on Fig. 5 G' *vs.* the reduced time $t/t_0(c_E)$, for $c_G = 5\%$. The various curves collapse into a single master one up to $t/t_0 \sim 3$–4. Beyond this scaling regime, they exhibit an ordered splay: the smaller c_E is, the slower the growth of G' on the scale of the initial pace of the reaction clock.

In the early, scaling regime, it appears (see insert of Fig. 5) that, except in a very narrow vicinity of the percolation threshold, G' grows quasi-linearly with t. We will show in Section III that in this regime gels with $c_G = 5\%$ present a weak level of

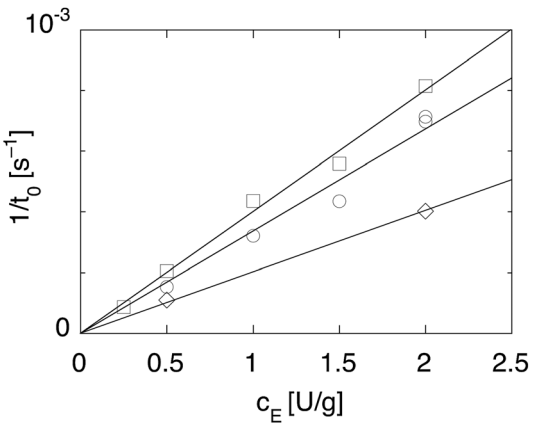

Fig. 4 Inverse gelation time *vs.* enzyme concentration for $c_G = 7.5\%$ (squares); 5% (circles); 3% (diamonds).

‡ We have found this criterion, although non standard, to be more reliable than the commonly used $G' = G''$ one, as the crossing value is often hardly larger than the noise level.

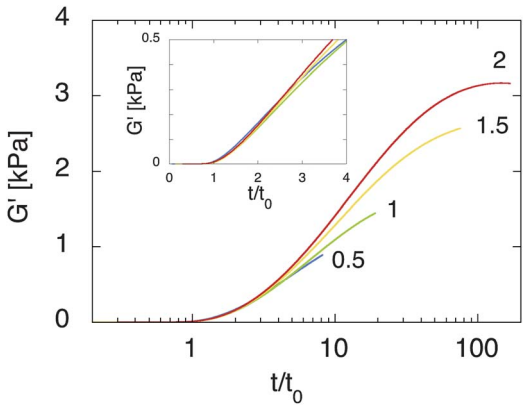

Fig. 5 Same data as Fig. 3 plotted *vs.* reduced time t/t_0. Inset: early gelation regime blow-up (lin-lin plot).

inhomogeneity. We therefore estimate their density of CLs ν on the basis of the expression for homogeneous gels. More precisely, for an affine network,[25] $G' = 2\nu k_B T$ where the factor of 2 accounts for the ratio between elastically active strand and CL densities. That is, the cross-linking rate per unit volume $\mathscr{R}$:

$$\mathscr{R} = \frac{d\nu}{dt} = \frac{1}{2k_B T}\frac{dG'}{dt} \tag{8}$$

Since, due to the scaling behavior, $G' \equiv \mathscr{G}(c_E t)$,

$$\mathscr{R}(c_E) = \frac{c_E}{\tau} \tag{9}$$

with c_E now expressed in number of E molecules per unit volume. Here τ is the enzyme "turnover time" in our gelled system, *i.e.* the average time interval between two successive reactions performed by the same E molecule.

From our data we estimate $\tau \approx 100$ s. This is to be contrasted with the turnover time of E, $\tau_{sol} \approx 0.1$ s deduced from the nominal activity of the enzyme for a non-polymeric substrate in solution (see Section 2). That is, even in this early regime, the geometric constraints imposed by the network result in a dramatic slowing down of the enzyme activity.

Effect of gelatin concentration. It is illustrated on Fig. 6, which displays the evolution of G' for systems with a fixed enzyme content $c_E = 2$ U g^{-1} and various gelatin concentrations ranging from 2 to 10%. Its build-up rate as well as its saturation value are seen to increase rapidly with c_G. The gelation time t_0 increases (see insert) as the gelatin content decreases and, as can be expected, this variation becomes more rapid for values $c_G \leq 2\%$, *i.e.* upon approaching the critical concentration, on the order of 1%.

We have checked (see Fig. 4) that the linear dependence of t_0^{-1} on the enzyme content c_E holds for the $c_G = 7.5\%$ gels as well as for the 5% ones. This leads us to investigate the range of validity of the scaling expression $G'(t, c_E) = \mathscr{G}(t/t_0(c_E))$ previously tested on the $c_G = 5\%$ gels. The result for $c_G = 3$, 5 and 7.5% is shown on Fig. 7. Comparison between the three panels immediately confirms the existence, for all three concentrations, of the scaling regime already identified for $c_G = 5\%$, extending over comparable ranges of reduced time, of order 3–4. As above, we can therefore evaluate a c_E-independent turnover time in the early gel phase, $\tau(c_G)$. The corresponding turnover rate $1/\tau$ is plotted on Fig. 8.

Finally, beyond the early scaling regime, for all c_G's, the curves on Fig. 7 exhibit a similar ordered splay. This departure from the scaling behavior indicates that, as the CL density grows, different paces for the reaction clock lead to different values of G' and hence, in all likelihood, to different network organizations. This points to the need for a complementary characterization of the gel structure.

3.2 Optical probing of network homogeneity

For each system composition, we have systematically monitored the time dependence of the spectral turbidity $\mathscr{T}(\lambda, t)$ in parallel with that of the elastic modulus. As a global characterization of the development of inhomogeneities of monomer concentration, we choose to first concentrate our attention on the growth of its value $\mathscr{T}^*(t)$ at wavelength 630 nm.

Fig. 9 displays, for a ($c_G = 5\%$, $c_E = 2$ U g^{-1}) system, the evolution of $\mathscr{T}^*$ along the course of gelation. It reaches a measurable level after a "latency time" $t_{\mathscr{T}}$ (here roughly comparable with the gelation one t_0). It then exhibits a continuous growth which parallels that of G', up to quite a significant level (in the case shown here $\sim$1cm^{-1}). Note, moreover, that in the late regime where G' has reached saturation, such is not the case for $\mathscr{T}^*$, which continues to grow logarithmically (see inset).

Effect of enzyme concentration. As shown on Fig. 10, corresponding to gels with $c_G = 5\%$ and various values of c_E, $t_{\mathscr{T}}$ increases as the enzyme concentration decreases, *i.e.* as t_0 grows.

This naturally leads us to plot $\mathscr{T}^*$ *versus* the reduced time $t/t_0(c_E)$ which previously arose from the analysis of the modulus data. Not only is the resulting collapse (see insert) excellent, but it extends up to $t/t_0 \sim 15$, *i.e.* much beyond the early gelation regime as defined on the basis of the scaling behavior of the

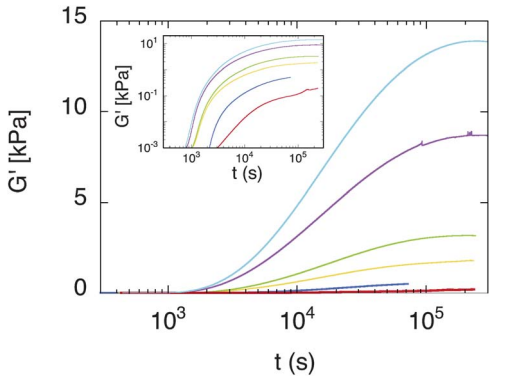

Fig. 6 Storage modulus build-up for $c_E = 2$ U g^{-1} and, from bottom to top, $c_G = 2$; 3; 4; 5; 7.5; 10%. Inset: log-log plot of the same data.

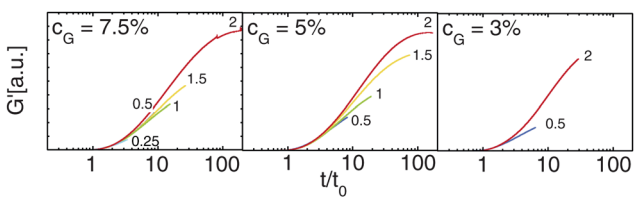

Fig. 7 Scaling plots $G'(t/t_0)$ for c_E values as labelled in U g^{-1}.

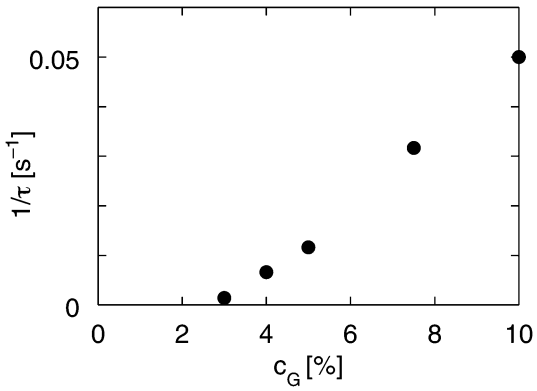

Fig. 8 Enzyme turnover rate $1/\tau$ (see text) *vs.* gelatin mass fraction.

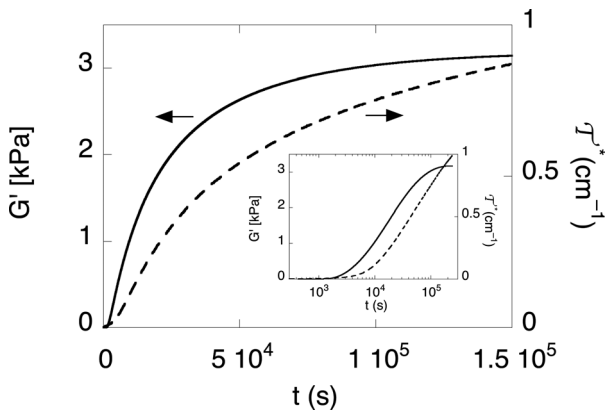

Fig. 9 Build-up of storage modulus G' (full line) and turbidity $\mathscr{T}^*$ (dashed line) of a ($c_G = 5\%$, $c_E = 2$ U g^{-1}) sample. Inset: log-lin plot of same data.

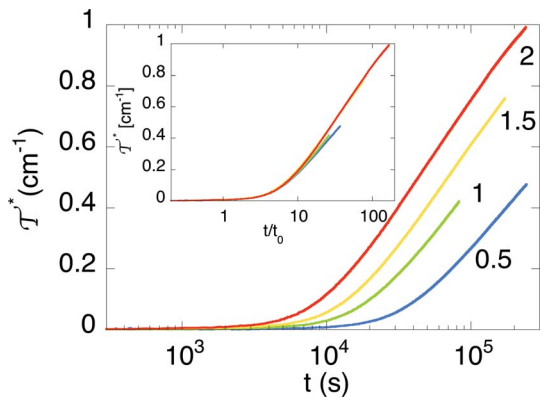

Fig. 10 Turbidity $\mathscr{T}^*$ *vs.* time for gels with fixed gelatin mass fraction $c_G = 5\%$ and enzyme concentrations as labelled. Insert: same data plotted *vs.* reduced time t/t_0.

modulus (see Fig. 5). A fully similar scaling behavior is also observed for gelatin concentrations $c_G = 7.5$ and 3%.

Dependence on gelatin concentration. As was found to be the case for G', at fixed enzyme concentration the turbidity turns out to depend strongly on the gelatin content.

Fig. 11 displays its evolution for gels with $c_G = 10$, 7.5, 5, 4, 3, 2%. The smaller c_G, the larger the $\mathscr{T}^*$ level, and the smaller the time of latency $t_{\mathscr{T}}$ preceding its emergence.

These trends are opposite to those found to characterize the behavior of G'—a statement illustrated on Fig. 12, which brings to light a strong anticorrelation between the modulus and turbidity levels.

Moreover, quite strikingly, the less concentrated the gel is, the more precocious the emergence of $\mathscr{T}^*$ with respect to that of G': while a 10% system gels before becoming turbid, a 2% one has become measurably turbid about 10^3 s before gelling. That is, upon increase of the gelatin content, the resulting gels evolve from weak-and-turbid to strong-and-clear.

Spectral turbidity. Turbidity not only depends on the number and optical contrast of the scatterers, but also on their size. Further insight into the evolution of the scale of concentration inhomogeneities can be derived from the wavelength dependence of $\mathscr{T}$. More precisely, the evolution with time of the "wavelength exponent" α (see Section 2) is shown on Fig. 13a for $c_E = 2$ U g^{-1} and various c_G values.

Assuming a simple model for spatial correlations (see Section 2) we extract from these data a rough evaluation of the scale d of the inhomogeneities. As seen on Fig. 13b, while for all systems d increases with time, its rate of growth is strongly c_G-dependent. For gels with $c_G \geq 5\%$, $d(t)$ is quasi-logarithmic and remains in the 10 nm range. For $c_G = 3$ and 4%, the growth is much faster (quasi-linear) and rapidly reaches values of order 100 nm. It should however be kept in mind that, as stressed in Aymard *et al.*,[7] these figures are of indicative value only.

Dynamic light scattering. Since many of the systems we have studied exhibit large $\mathscr{T}$ values, there obviously is a need for establishing, at least empirically, a criterion for what can be considered a small turbidity range—*i.e.* the $\mathscr{T}$ range in which results from the theory of homogeneous gels can be safely made use of. We have resorted for this purpose to DLS experiments, from which we extract values of the collective diffusion coefficient D_{coll}, which characterizes the relative motion of the network and solvent. Fig. 14a displays the evolution of D_{coll} as gelation proceeds.

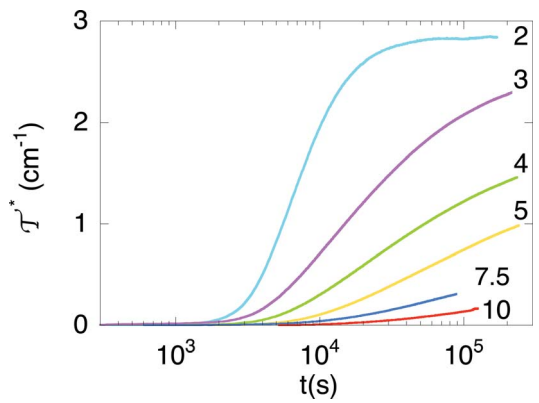

Fig. 11 Build-up of turbidity $\mathscr{T}^*$ for systems with $c_E = 2$ U g^{-1} and gelatin concentrations c_G as labelled (in %).

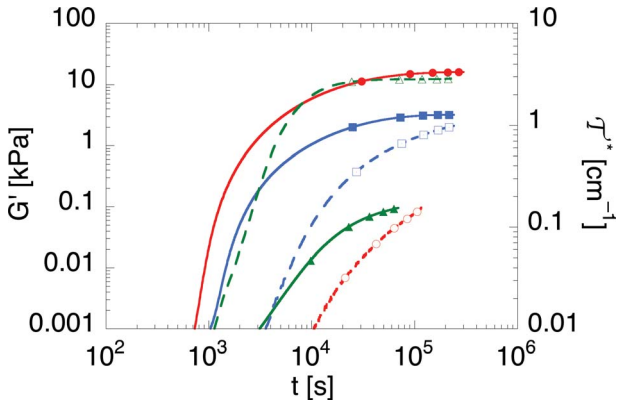

Fig. 12 Evolution of shear modulus G' (full lines) and turbidity $\mathcal{T}^*$ (dashed lines) for $c_E = 2$ U g^{-1} and gelatin content $c_G = 2\%$ (green, triangles), 5% (blue, squares), 10% (red, circles).

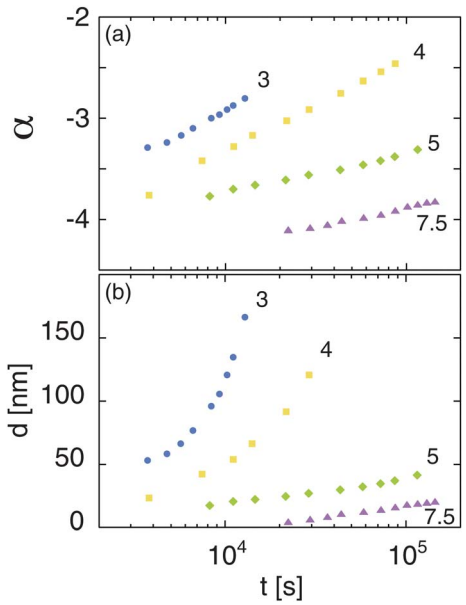

Fig. 13 Time evolution of the turbidity wavelength exponent α (a) and of the inhomogeneity lengthscale d (b) for systems with $c_E = 2$ U g^{-1} and c_G as labelled.

The continuum mechanics description of homogeneous gels leads to introducing a Darcy-like porosity κ which controls their poroelastic properties, associated with relative motions of the solvent and the network. For a gel of mesh size ξ, $\kappa \sim \xi^2$ and

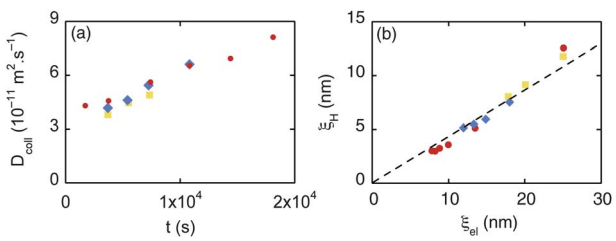

Fig. 14 (a) Collective diffusion coefficient D_{coll} *vs.* time for $c_E = 2$ U/g, $c_G = 10\%$(red dots); 7.5% (blue diamonds); 5% (yellow squares). (b) Hydrodynamic *vs.* elastic estimates of the network mesh size for the same systems as left panel.

$D_{coll} \simeq G'\kappa/\eta_s$ with η_s the solvent viscosity.[26] From this we define a hydrodynamic estimate of the mesh size:

$$\xi_H = \left(\frac{D_{coll}\eta_s}{G'}\right)^{1/2} \tag{10}$$

On the other hand, for a network with entropic elasticity, a elastic estimate is:[27]

$$\xi_{el} = \left(\frac{k_B T}{G'}\right)^{1/3} \tag{11}$$

We check that both lengths decrease as cross-linking proceeds. Furthermore if gel inhomogeneity is negligible, these two lengths should scale as the mesh size itself, hence should be proportional to each other.[28] Fig. 14b shows that, in the turbidity range $\mathcal{T}^* < 0.1$ cm^{-1} to which our DLS measurements are restricted (see section 2), this is indeed the case.

This justifies *a posteriori* our above evaluations of the rate of cross-linking in the early stage of gelation.

4 Discussion

Enzyme kinetics in the gel phase

Tgase-mediated cross-linking is a two-step reaction. In the first one, S_1, the amide group of a glutamine (Gln) is cleaved, which results in the formation of an acyl-enzyme complex (EGln). In the second step S_2, the ε-amino group of a lysine (Lys) binds to (EGln), then the CL is formed and the Tgase is released. For enzymatic reactions in solution—*i.e.* in the absence of geometric constraints on the motion of the participating species—the standard kinetic model is the Michaelis–Menten (MM) one.[29] Its extension to the case of our two-step reaction (see Appendix) results in the following expression for the rate of CL production $d[CL]/dt = \mathcal{R}_{MM}$:

$$\mathcal{R}_{MM} = c_E \frac{k_{cat}[Gln][Lys]}{[Gln][Lys] + K_m[Lys] + K'_m[Gln]} \tag{12}$$

where k_{cat}, K_m and K'_m depend only on the kinetic constants involved in $S_{1,2}$ (and square brackets indicate concentrations). We also show in the Appendix that, within the extended MM-scheme, the concentrations of the substrates (Gln and Lys) and product (CL) are functions of ($c_E t$) and c_G only. That is, the value of the enzyme concentration simply sets the "pace of the reaction clock".

How these kinetics are modified when the reaction takes place in a constrained and/or crowded gel-like medium (such as the extra-cellular matrix) remains a fully open question. In particular, to what extent does the linearity in the enzyme concentration remain valid in our system as gelation proceeds?

We have seen that measurements of $G'(t)$ give us access to the cross-linking rate in the gel phase, $\mathcal{R}$, *via* eqn (8), provided that the turbidity $\mathcal{T}^* \lesssim 0.1$ cm^{-1}. The extent of this regime increases when c_G grows. Let us first concentrate on the case $c_G = 10\%$ for which the small $\mathcal{T}^*$ condition holds up to full gelation.

As discussed in the previous section, in the early gelation regime extending from $\sim t_0$ to $\sim 4t_0$, the number of CL's grows linearly with time. Beyond this, the reaction rate decreases over a range $\sim 200t_0$ down to negligibly small values. The

corresponding saturation modulus $G'_{sat} \simeq 16$ kPa. From this we evaluate the CL concentration $\nu_{sat} = G'_{sat}/2k_BT \simeq 3.3$ mM. This is to be compared with the total amount of lysine—the less abundant substrate—in the system, namely [Lys] = 33 mM. That is, at saturation, about 10% only of the candidate CL have been formed. So, gelation stops due, not to substrate exhaustion, but to kinetic slowing down.

For smaller c_G's, down to about 3%, the small $\mathscr{T}^*$ condition only holds in the early gelation regime where we were able to determine the turnover time of a Tgase molecule $\tau(c_G)$. It decreases as c_G grows (see Fig. 8) and ranges from $\tau(3\%) = 700$ s to $\tau(10\%) = 16$ s. These values are huge compared to the turnover time $\tau_{sol} \simeq 0.1$ s obtained from the test of activity in solution. This is certainly to be related to the fact that the emergence of a finite G' signals the percolation of preformed gel clusters which have been growing in size and number during the pre-gelation latency period—so that early gelation has nothing in common with the onset of cross-linking where eqn (12) is likely to apply with [Gln] and [Lys] given by their initial values, proportional to c_G. That early gelation lies far out of the range of validity of the MM description is confirmed by the observation (see Fig. 8) that the growth of the turnover rate $1/\tau$ with c_G is faster than linear, in particular at the lower gelatin concentrations. Indeed, at the onset of cross-linking, $\mathscr{R}_{MM} \sim c_E c_G/(c_G + K)$ *i.e.* grows sub-linearly with c_G.

This leads us to stress that, even when the substrate is rather dilute and elastically very weak, it is by no means legitimate to analyze the kinetics of the enzyme-mediated reaction in the frame of a standard MM model.

Origin of the kinetic slowing down

Let us first focus on step S_1 of the cross-linking reaction. Slowing down may affect either the transport process or the reaction between E and Gln itself. One may of course wonder whether the decrease with time of the mesh size could result in a gradual restriction of the diffusive motion of the enzyme, ultimately leading to its "caging". The hydrodynamic radius of a Tgase molecule can be estimated as 2.7 nm.[30] Fadda *et al.*[30] have shown that a passive particle of hydrodynamic radius R_H within a gel of mesh size $\sim 4R_H$ diffuses freely but experiences an effective viscosity enhancement by a factor ~ 8. This corresponds for Tgase to a mesh size $\simeq 10$ nm, *i.e.* to $G' \simeq 4$ kPa. For all our gels, the early regime corresponds to moduli smaller than this value. Therefore, the reduction of the diffusion coefficient due to crowding could at best account for a few percent of the value of the slowing down factor in the early regime $\tau/\tau_{sol} \sim 160$–7000. It is only for concentrated gels close to saturation that crowding might become relevant.

We must thus primarily assign the global slowing down to that of the motion of the gelatin residues (and of the EGln complex) as the mesh size decreases. Indeed, the geometrical constraints imposed by the network severely reduce both their translational and rotational mobilities. Given the high orientational selectivity of the reactions under consideration, it is certainly the freezing out of rotational degrees of freedom which is most efficient in this respect—and even more so for the reaction in step S_2, the two partners of which are attached to the network, instead of only one of them in step S_1.

Therefore, in all likelihood, it is the second reaction which is limiting for the kinetics. An analogous conclusion has been demonstrated by Abete *et al.*[31] in their interpretation of the study by Hellio-Serughetti and Djabourov[32] on the chemical gelation of gelatin with the help of a consumed cross-linking agent. In this perspective, note that we have evaluated, for the $c_G = 10\%$ gel at saturation, a mesh size ~ 7 nm—comparable with the persistence length of gelatin.[33] In this extreme situation, rotations should be quasi-forbidden, which is consistent with the vanishing of the cross-linking rate.

Chemo-osmotic coupling and inhomogeneity amplification

We must now address the question of the physical origin and dynamics of inhomogeneity development in our system. It is of course well known that chemical gels are quasi-inevitably inhomogeneous.[34] In many cases this can be attributed to the fact that their chemical kinetics are too fast to permit proper homogenization of the pregel solution. This is for instance the case for alginate chain cross-linking by free Ca^{2+} ions.[35] Here, the ultra-slow rate we measure for enzymatic cross-linking ensures that we are rid of this "exogenous" source of disorder.

On the other hand we have seen that, systematically:

(i) as gelation proceeds, the build-up of the shear modulus G' is indissociable from that of the optical turbidity $\mathscr{T}^*$.

(ii) The dependence of G' and $\mathscr{T}^*$ on c_G are strongly anti-correlated. Not only does an increase of c_G induce an increase (resp. decrease) of the G' (resp. $\mathscr{T}^*$) level, but also a decrease (resp. increase) of the emergence time t_0 (resp. latency time $t_{\mathscr{T}}$).

This leads us to conclude that we are dealing here with the result of a physical mechanism of amplification, by the cross-linking reaction, of the statistical fluctuations of the network structure.

a. Basic mechanism. Indeed, consider for instance that some region of space is the seat of a positive fluctuation of monomer density ($\delta c_G > 0$). Since the enzyme reaction rate $1/\tau$ increases notably with c_G, this induces a positive fluctuation of the CL density ($\delta\nu > 0$) with respect to the surrounding medium.

In order to make this more explicit, let us consider the following simple model: a gel is prepared from a polymer solution of homogeneous monomer concentration but with a small, 1-D stepwise CL density fluctuation. As prepared, the system is supposed to be in its mechanical reference state. Clearly, such a system is the seat of an osmotic imbalance that will induce a displacement of the plane separating the stiffer and looser regions (see Fig. 15), so as to minimize the total free energy of the system at constant total volume. Without much loss of generality

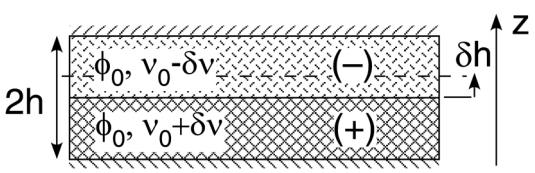

Fig. 15 Schematic configuration of a sample with a 1-D stepwise CL density fluctuation.

one can consider that the initial step is equidistant from the boundaries of the sample.

The Flory–Rehner free energy of each homogeneous region ($i = +, -$) of initial volume V_0, monomer volume fraction ϕ_0 and CL density ν_i, reads:[36]

$$\frac{\mathscr{F}_i}{k_B T} = \frac{\alpha_i V_0}{w}(1/2 - \chi)\frac{\phi_0^2}{\alpha_i^2} + \nu_i V_0\left[\frac{\alpha_i^2 - 1}{2} - B\ln\alpha_i\right] - c_0^{ion} V_0 \ln\alpha_i \quad (13)$$

$\alpha_\pm = 1 \pm \delta h/h$ is the stretching ratio along direction z. The first term on the right-hand side is the leading relevant term of the energy of mixing, with w the volume of both solvent molecules and monomers and χ the Flory parameter. Under good solvent conditions, which we assume here, $\chi < 1/2$. The second term is the elastic contribution of the stretched network, the ln term accounting for the entropy of the CLs. The last term is the contribution of the counter-ions, c_0^{ion} their number per unit volume in the reference state. In our case, where the solvent is pure water, the ions are provided by the gelatin itself, so that $c_0^{ion} = A\phi_0$ is proportional to the monomer density. Note that such would not be the case for a buffered solution.

The equilibrium at fixed volume is given by $\varpi_+ = \varpi_-$ where

$$\varpi_i = -\frac{1}{V_0}\frac{\partial \mathscr{F}_i}{\partial \alpha_i} \quad (14)$$

is the swelling pressure, *i.e.* the difference between the osmotic pressure, which causes the polymer chains to expand, and the elastic pressure from the network, which tends to make them contract.[37]

With $\delta\alpha = \delta h/h \ll 1$, the equilibrium condition reads:

$$\frac{\delta\alpha}{\delta\nu} = -\frac{1 - B}{C\phi_0^2 + A\phi_0 + (1 + B)\nu_0} \quad (15)$$

with $C = (1 - 2\chi)/w > 0$. Therefore, the sign of the restoring osmotic flow is that of $B - 1$. The value of B, originally predicted to be 1, has been a subject of controversy and different values has been proposed, all such that $B \leq 1$. Some authors[38] even omit this term ($B = 0$). We therefore conclude that, generically, the swelling pressure difference drives the solvent out ($\delta\alpha < 0$) of the more densely cross-linked region ($\delta\nu > 0$) into the looser one. Since the cross-linking rate increases with substrate concentration, this microsyneresis[39] response then induces a further increase of the initial $\delta\nu$.

Two conditions must be satisfied for this positive feedback mechanism to act as an efficient source for the development of optically observable inhomogeneities:

(i) Cross-linking must be an irreversible process: indeed, physical gels exhibit substantial stress relaxation which counteracts the growth of stress inhomogeneities *via* CL rearrangement. This probably explains why thermoreversible gelatin gels exhibit negligible turbidity compared with chemical ones.

(ii) The cross-linking reaction must be slow enough with respect to the time scale of solvent diffusive transport on length scales of at least a few 10 nm. This can be put on a more quantitative footing: the diffusion time for the flow of solvent out of an inhomogeneity of radius R is $T_{diff} \sim R^2/D_{coll}$. It must be smaller than the time for creating one extra CL in a volume $\sim R^3$, *i.e.* (from eqn (9)) $T_{CL} \sim (\mathscr{R}(c_E)R^3)^{-1}$. This condition is fulfilled for inhomogeneities smaller than:

$$R^* \sim (D_{coll}/\mathscr{R})^{1/5} \quad (16)$$

Due to the 1/5 power R^* lies, for all our systems, in the very narrow range 1–2.5 μm. We are thus led to conclude that Tgase-mediated cross-linking is slow enough for the amplification mechanism to be fully efficient for optically active inhomogeneities.

In order to check that osmotic transport up to the micrometre scale is effectively "slaved" to the reaction kinetics, we have performed the following control experiment. We let a $c_G = 3\%$ system gel for about 10^4 s. This value is chosen to lie in the early gelling regime, so that the rates of variation of G' and $\mathscr{T}^*$ still have their maximum values. We then inactivate the enzyme (see Section 2), after which we bring temperature back to its initial value.

Fig. 16 shows that, over the subsequent 10^5 s, the modulus remains constant, which proves the effectiveness of the inactivation process. Moreover, turbidity "freezes" without exhibiting any measurable transient. That is, inhomogeneity development adapts quasi-instantaneously to the state of cross-linking.

b. A complementary mechanism. The only condition for the above mechanism to operate (whatever its efficiency) is that the reaction rate be an increasing function of the substrate concentration c_G—which should be the case for most interchain cross-linking processes. Beyond this, the possibility of another, much more system-specific, source of inhomogeneity growth should be kept in mind. Namely, as was suggested already long ago,[39] one cannot rule out that the Flory parameter χ would increase with the CL density ν, making the solvent poorer and poorer as the gel stiffens, possibly so much as to cross the spinodal limit where linear instability is reached.

Gelatin in water is a good candidate for such a behavior. Indeed, slightly above the physical gelling temperature, its χ value was shown to be 0.49.[40] This value, very close to the θ-solvent frontier, probably reflects the trend of gelatin to forming the intra-chain H-bonds responsible for the formation of helix structures. The formation of a chemical CL is likely to prevent the screening of hydrophobic interactions on the scale of the persistence length, which is here quite sizeable (~2 nm).

This effect, if present, reinforces the previously described heterogeneity amplification mechanism, by increasing the

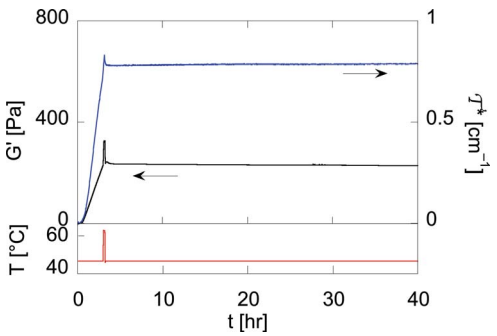

Fig. 16 Upper panel: Effect of thermally-induced enzyme inactivation on the shear modulus G' and turbidity $\mathscr{T}^*$ of a $c_G = 3\%$, $c_E = 2$ U g^{-1} gel. The lower panel shows the thermal history.

swelling pressure difference which pushes water out of the stiffer regions into the looser ones.

Comparison with main experimental features

We must now assess whether our proposed scenario is consistent with the most salient features of our experimental results.

The first observation to be accounted for is the systematic anti-correlation between the modulus and turbidity levels as the gelatin content is varied, summed up on Fig. 17.

Let us refer to eqn (15) in which, disregarding the density difference between monomer and solvent, we identify ϕ_0 with the gelatin concentration c_G. We found that the larger c_G, the higher the cross-linking rate, that is, at a given time, the larger ν_0. Hence, the denominator of $\delta\alpha/\delta\nu$ increases with c_G, *i.e.* the amplification effect decreases. So the chemo-osmotic mechanism does predict a global negative correlation between cross-linking and inhomogeneity levels.

For a given c_G, as time elapses ν_0 increases, which explains the observed slowing down of the turbidity growth. On the other hand, we have noticed (see inset of Fig. 9) that, while at large times G' saturates, $\mathscr{T}^*$ continues to grow slowly (quasi-logarithmically). This, when contrasted with the behavior following enzyme inactivation (see Fig. 16), shows that the cross-linking rate has not vanished. In this late stage, the gel has developed marked stiffness inhomogeneities, so that the G' value is no longer simply controlled by the average CL density. The fact that $\mathscr{T}^*$ still increases proves that, although the enzyme activity is globally slowed down due to the mesh size decrease, it remains larger in the denser regions. The negligible sensitivity of G' to the stiffening of these clusters moreover suggests that (i) they do not percolate and (ii) they exhibit quite large stiffness contrast with the average embedding medium.

The last striking qualitative observation is that, for dilute systems, turbidity emerges prior to modulus. This clearly demonstrates that the chemo-osmotic mechanism is already at work in the pregel phase. Moreover, as long as the size of the microgel clusters remains smaller than the cut-off length R^* defined by eqn (16), it leads to cluster shrinking, hence hinders percolation. Indeed, we have been able to prepare a $c_G = 1.5\%$ system which still flows as a liquid but exhibits a turbidity higher than 1 cm^{-1}, *i.e.* looks as milky as the sample shown on Fig. 1.

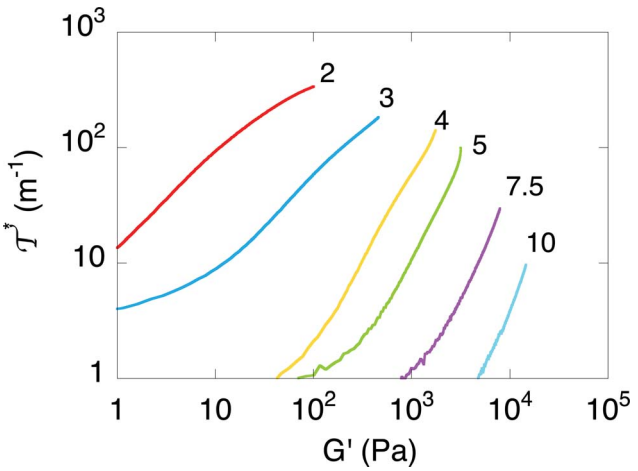

Fig. 17 Turbidity $\mathscr{T}^*$ *vs.* shear modulus G' during gelation of $c_E = 2$ U g^{-1} systems with c_G values as labelled (same data as Fig. 6 and Fig. 11).

5 Conclusion

We believe the work presented here to be the first case where it has been possible to quantitatively study the development of inhomogeneities during the course of the chemical gelation of a solution of preexisting polymers which, contrary to *e.g.* agarose, is not the seat of a demixing instability. This is made possible by the extreme slowness of the enzyme-mediated cross-linking kinetics, which turns out to present a twofold advantage. On the one hand one can easily monitor the build-up of both rheological and optical characteristics. More importantly, it is this slowness itself which is responsible for the high efficiency of the inhomogeneity amplification mechanism. Indeed, we have shown that this consists of feedback between (i) the positive dependence of the bridging rate on the polymer concentration (ii) the osmotic flow triggered by the resulting increase of cross-link density. To our knowledge, it is the first time that microsyneresis is proved to be at work in a thermodynamically stable system. The chemo-osmotic mechanism is sufficient to explain the qualitative features of our results. Nevertheless, we cannot exclude that it would be assisted[27] by the decrease of solvent quality induced by the creation of cross-links itself.

A natural extension of this study will be to compare the behavior of chemical gelatin gels obtained either *via* enzymatic catalysis or by slow interchain bridging with the help of a consumed reactant.[32]

Appendix

The two-step scheme of the cross-linking reaction can be written as follows:

$$\mathrm{E} + \mathrm{Gln} \underset{k_{-1}}{\overset{k_1}{\rightleftharpoons}} \mathrm{X}^{\ddagger} \xrightarrow{k_2} \mathrm{EGln} + \mathrm{NH_3} \qquad \text{(S1)}$$

$$\mathrm{EGln} + \mathrm{Lys} \underset{k'_{-1}}{\overset{k'_1}{\rightleftharpoons}} \mathrm{Y}^{\ddagger} \xrightarrow{k'_2} \mathrm{E} + \mathrm{CL} \qquad \text{(S2)}$$

where $X^{\ddagger}$ and $Y^{\ddagger}$ designate the transition states of steps S_1 and S_2. EGln stands for the intermediate acyl-enzyme complex and CL for the final cross-link. The extension of the standard Michaelis–Menten approach to the two-step case amounts to neglecting the time variations of the intermediate product concentrations [$X^{\ddagger}$], [EGln] and [$Y^{\ddagger}$].[29] The condition for this steady state approximation to be legitimate is that the substrate concentrations [Gln] and [Lys] are much larger than the initial enzyme one c_E. We saw in Section IV that this condition is always fully satisfied in our gels.

Exploiting the steady state conditions $d[X^{\ddagger}]/dt = d[\mathrm{EGln}]/dt = d[Y^{\ddagger}]/dt \simeq 0$, and using the stoichiometric relationship $c_E = [E] + [X^{\ddagger}] + [\mathrm{EGln}] + [Y^{\ddagger}]$, one obtains after some algebra:

$$\frac{d[\mathrm{CL}]}{dt} = c_E \frac{k_{cat}[\mathrm{Gln}][\mathrm{Lys}]}{[\mathrm{Gln}][\mathrm{Lys}] + K_m[\mathrm{Lys}] + K'_m[\mathrm{Gln}]} \qquad (17)$$

with

$$k_{\mathrm{cat}} = \frac{k_2 k_2'}{k_2 + k_2'} \tag{18}$$

$$K_{\mathrm{m}} = \frac{k_2'(k_{-1} + k_2)}{k_1(k_2 + k_2')} \tag{19}$$

$$K_{\mathrm{m}}' = \frac{k_2\left(k_{-1}' + k_2'\right)}{k_1'(k_2 + k_2')} \tag{20}$$

Moreover, since the concentrations of intermediate products are stationary, the consumption rates of both substrates (Gln and Lys) are simply the opposite of the rate of cross-linking:

$$\frac{d[\mathrm{Gln}]}{dt} = \frac{d[\mathrm{Lys}]}{dt} = -\frac{d[\mathrm{CL}]}{dt} \propto c_{\mathrm{E}} \tag{21}$$

with the initial concentrations $[\mathrm{Gln}]_0 = \alpha_{\mathrm{Gln}} c_{\mathrm{G}}$ and $[\mathrm{Lys}]_0 = \alpha_{\mathrm{Lys}} c_{\mathrm{G}}$. It is therefore clear that, as long as the Michaelis–Menten approximation holds, [CL] (as well as [Gln] and [Lys]) is a function of c_{G} and $t' = c_{\mathrm{E}} t$ only. Since for a given c_{G}, the percolation threshold corresponds to a c_{E}-independent value ν_0 of [CL], it is thus reached at a time $t_0(c_{\mathrm{E}}) \sim c_{\mathrm{E}}^{-1}$. Accordingly, [CL]($t$) is expected to be a unique function of the reduced time t/t_0.

Acknowledgements

We are indebted to W. Helbert and J.-F. Joanny for stimulating discussions. H.S. is grateful to R. Agniel for technical assistance. We acknowledge funding from Émergence-UPMC-2010 research program.

References

1 J. L. Drury and D. J. Mooney, *Biomaterials*, 2003, **24**, 4337–4351.
2 J. Gong and Y. Osada, In High Solid Dispersions, M. Cloitre, Ed., *Adv. Polym. Sci.*, Springer, 2010, 236, 203–246.
3 G. Miquelard-Garnier, D. Hourdet and C. Creton, *Polymer*, 2009, **50**, 481–490.
4 F. Ikkai and M. Shibayama, *J. Polym. Sci., Part B: Polym. Phys.*, 2005, **43**, 617–628.
5 K. te Nijenhuis, Thermoreversible networks: viscoelastic properties and structure of gels, *Adv. Polym. Sci.*, Springer, 1997, 130, 1–235.
6 S. Giraudier, D. Hellio-Serughetti, M. Djabourov and V. Larreta-Garde, *Biomacromolecules*, 2004, **5**, 1662–1666.
7 P. Aymard, D. R. Martin, K. Plucknett, T. J. Foster, A. H. Clark and I. T. Norton, *Biopolymers*, 2001, **59**, 131–144.
8 G. Feke and W. Prins, *Macromolecules*, 1974, **7**, 527–530.
9 P. S. Biagio, D. Bulone, A. Emanuele, M. Palma-Vittorelli and M. Palma, *Food Hydrocolloids*, 1996, **10**, 91–97.
10 H. Nakazawa and K. Sekimoto, *J. Chem. Phys.*, 1996, **104**, 1675–1683.
11 G. O. Phillips and P. A. Williams, *Handbook of Hydrocolloids*, CRC Press, Cleveland, 2000.
12 V. Crescenzi, A. Francescangeli and A. Taglienti, *Biomacromolecules*, 2002, **3**, 1384–1391.
13 T. Kashiwagi, K.-i. Yokoyama, K. Ishikawa, K. Ono, D. Ejima, H. Matsui and E.-i. Suzuki, *J. Biol. Chem.*, 2002, **277**, 44252–44260.
14 M. Motoki and K. Seguro, *Trends Food Sci. Technol.*, 1998, **9**, 204–210.
15 L. Cui, G. Du, D. Zhang, H. Liu and J. Chen, *Food Chem.*, 2007, **105**, 612–618.
16 M. M. Bradford, *Anal. Biochem.*, 1976, **72**, 248–254.
17 sodium dodecyl sulfate polyacrylamide gel electrophoresis, see U. K. Laemmli, *Nature*, 1970, **227**, 680–685.
18 M. S. Lantz, P. Ciborowski, In Bacterial Pathogenesis Part A: Identification and Regulation of Virulence Factors, Virginia L. Clark, P. Bavoil, J. Abelson and M. Simon Ed., *Method. Enzymol.*, Academic Press, 1994, 235, 563–594.
19 M. Harz and M. Knoche, *Crop Prot.*, 2001, **20**, 489–498.
20 H. van de Hulst, Light scattering by small particles, *Structure of Matter Series*; Dover Publications, 1957.
21 M. Shibayama, *Bull. Chem. Soc. Jpn.*, 2006, **79**, 1799–1819.
22 J.-Z. Xue, D. J. Pine, S. T. Milner, X.-l. Wu and P. M. Chaikin, *Phys. Rev. A: At., Mol., Opt. Phys.*, 1992, **46**, 6550–6563.
23 T. Tanaka, L. O. Hocker and G. B. Benedek, *J. Chem. Phys.*, 1973, **59**, 5151–5159.
24 S. Giraudier and V. Larreta-Garde, *Biophys. J.*, 2007, **93**, 629–636.
25 M. Rubinstein and R. Colby, *Polymer physics*; Oxford University Press, 2003.
26 D. L. Johnson, *J. Chem. Phys.*, 1982, **77**, 1531–1539.
27 P. G. de Gennes, *Scaling Concepts in Polymer Physics*, Cornell University Press: Ithaca, 1979.
28 T. Baumberger, C. Caroli and O. Ronsin, *Eur. Phys. J. E*, 2003, **11**, 85–93.
29 A. Cornish-Bowden, *Fundamentals of enzyme kinetics*, 3rd ed., Portland Press, 2004.
30 G. Fadda, D. Lairez, B. Arrio, J.-P. Carton and V. Larreta-Garde, *Biophys. J.*, 2003, **85**, 2808–2817.
31 T. Abete, E. D. Gado, D. Hellio-Serughetti, L. de Arcangelis, M. Djabourov and A. Coniglio, *J. Chem. Phys.*, 2006, **125**, 174903.
32 D. Hellio-Serughetti and M. Djabourov, *Langmuir*, 2006, **22**, 8509–8515.
33 I. Pezron, M. Djabourov and J. Leblond, *Polymer*, 1991, **32**, 3201–3210.
34 J. Bastide and S. Candau, In *Physical Properties of Polymeric Gels*, J. Cohen Addad Ed., J. Wiley, 1996, 143–308.
35 I. Donati and S. Paoletti, In Alginates: Biology and Applications; B. H. A. Rehm Ed., *Microbiology Monographs*, Springer, 2009, 13, 1–53.
36 A. Onuki, *Phase Transition Dynamics*, Cambridge University Press, 2002.
37 E. Geissler, A.-M. Hecht and F. Horkay, *J. Macromol. Sci., Part B: Phys.*, 2005, **44**, 873–880.
38 M. Doi, *J. Phys. Soc. Jpn.*, 2009, **78**, 052001.
39 K. Dušek and W. Prins, Fortschritte der Hochpolymeren-Forschung, *Adv. Polym. Sci.*, Springer, 1969, 6, 1–102.
40 H. B. Bohidar and S. S. Jena, *J. Chem. Phys.*, 1994, **100**, 6888–6895.